Optica Applicata, Vol. XXI, No. 1, 1991

On the possibility of sphero-chromatic aberration correction of single holo-lens used as a spectral device

M. ZAJĄC, J. NOWAK, B. DUBIK

Institute of Physics, Technical University of Wrocław, Wybrzeże Wyspiańskiego 27, 50-370 Wrocław, Poland.

Considerable chromatic aberration characterizing holographic lens can be used to design a simple spectral device in which a holo-lens acts as focusing and dispersive element at the same time. For optimizing the geometry parameters of such a device, it is necessary to analyse the sphero-chromatic aberration of single holo-lens. In the paper, the conditions for simultaneous vanishing of both spherical aberration and its first derivative are determined. To verify the obtained relations polychromatic images of point object are evaluated by means of numerical modelling of imaging for some exemplary imaging configurations.

1. Introduction

Holographic optical elements (HOE) become more and more important in modern optics [1]–[4]. Their aberration properties are well known and described in many publications. Most of the papers are limited to the investigations in a monochromatic light beacuse of the significant chromatic aberration of these elements. This specific feature of holographic lens can be, however, profitable property of such optical elements and may allow us to apply holographic lens as a part of spectral device, e.g., monochromator, spectroscope, fiber optical multiplexer [5]–[8], and others.

From this point of view, it is necessary to investigate the chromatic properties of such a holographic element in a full visible light range.

In most cases a point object located on axis is of interest to us. Taking into account small field angles it seems to be sufficient to start from the aberration analysis according to MEIER approximation [9]. Nevertheless, it is obvious that for full analysis of imaging quality the third order aberration description is not sufficient. In order to have real intensity distribution in an aberration spot a numerical simulation of holographic lens imaging can be used [10].

2. Correction of sphero-chromatic aberration

2.1. Analytical formulae

Let us consider a holographic lens (holo-lens) recorded according to the geometry shown in Fig. 1a. Symbols P_α and P_β denote point sources of spherical waves creating the holo-lens; z_α and z_β are the respective distances from those points to the

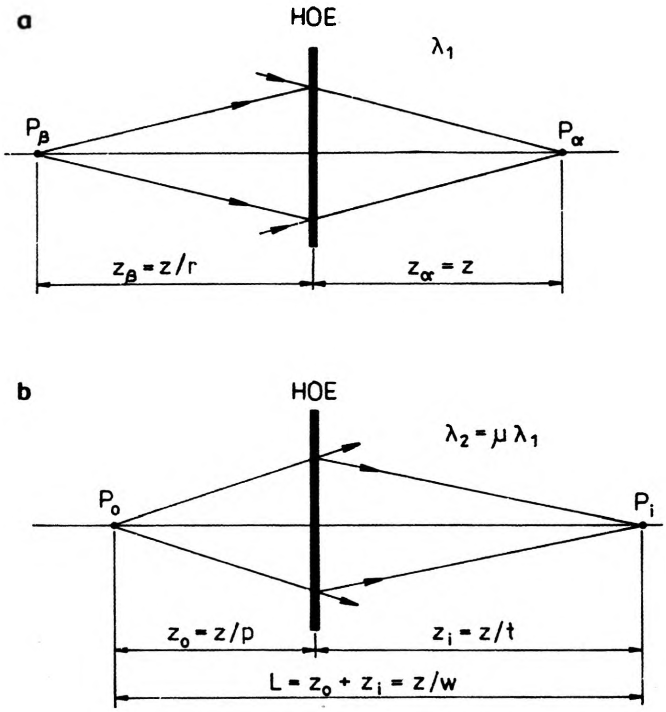

Fig. 1. Holo-lens recording geometry (a), and imaging geometry (b)

holo-lens plane. The light wavelength used during the recording step is λ_1. This holo-lens is used to image a point object P_o located on axis in the distance z_o in front of it, as it is shown in Fig. 1**b**. The light wavelength λ_2 used in this step is in general different than λ_1 and $\lambda_2/\lambda_1 = \mu$. The image P_i is observed on axis in Gaussian plane situated in the distance z_i behind the holo-lens. The value of z_i depends on the distances z_α, z_β, z_o and parameter μ as follows (signs +, − correspond to the primary or secondary image, respectively)

$$1/z_i = 1/z_o \pm \mu(1/z_\alpha - 1/z_\beta). \tag{1a}$$

To simplify the notation, undimensional parameters: z, r, p, t, w describing the recording and imaging geometries, are introduced (see Fig. 1**a**, **b**).

$$t = p \pm \mu(1-r). \tag{1b}$$

It means that for the given position of a point object and observation plane (fixed p and t) a sharp image is formed only for one particular wavelength; the other wavelengths give smeared and low intensity images in this plane. On the other hand, for every wavelength there exists an observation plane (defined by parameter t), where the Gaussian image relation (1) is fulfilled. This particular wavelength will be called "base" for a given pair of distances z_o and z_i (i.e., parameters p and t). Therefore, by shifting the observation plane along the axis perpendicular to the holo-lens the light wavelength can be selected.

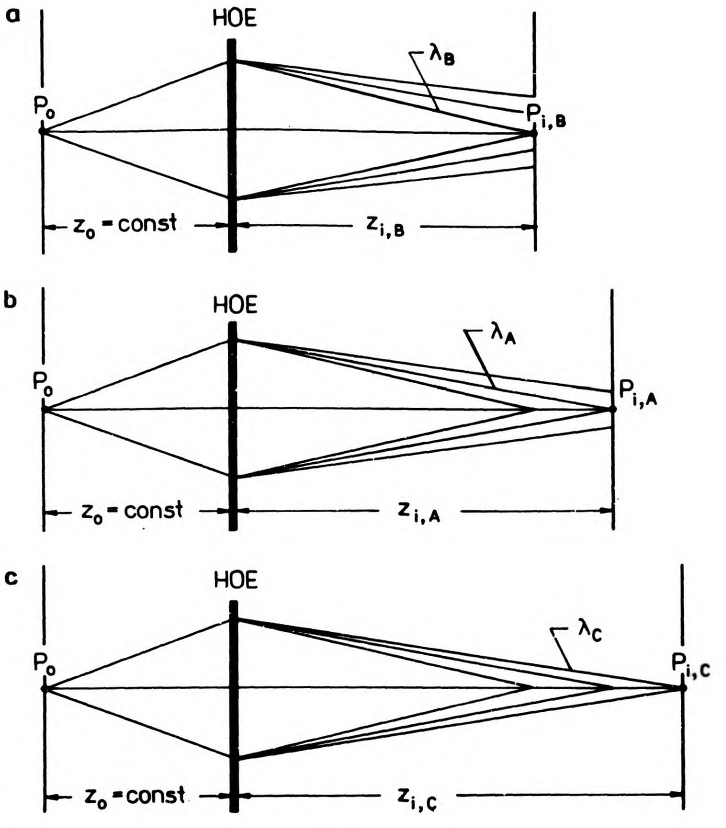

Fig. 2. Schematic diagram of spectral device in configuration No. 1: **a** – geometry B, **b** – geometry A, **c** – geometry C

As the object point P_o is located on axis then all third-order aberrations except the spherical one are equal to zero. The spherical aberration coefficient S depends on the holo-lens recording parameters z_α, z_β, μ and object distance z_o as follows [9]:

$$S = 1/z_o^3 \pm \mu(1/z_\alpha^3 - 1/z_\beta^3) - 1/z_i^3. \tag{2a}$$

The same relation can be expressed using undimensional parameters r, z, p, μ

$$S = [p^3 \pm \mu(1-r^3) - t^3]/z^3. \tag{2b}$$

The aberration coefficient S is a function of parameter μ

$$S(\mu) = \pm[1-r^3]\mu^3 - [3p(1-r)^2]\mu^2 \pm [1-r^3-3p^2(1-r)]\mu. \tag{2c}$$

The following analysis is conducted independently for two different ways of changing the "base" wavelength called configuration No. 1 and configuration No. 2.

2.2. Configuration No. 1

The imaging geometry of fixed object distance $z_o = \text{const}$ will be called

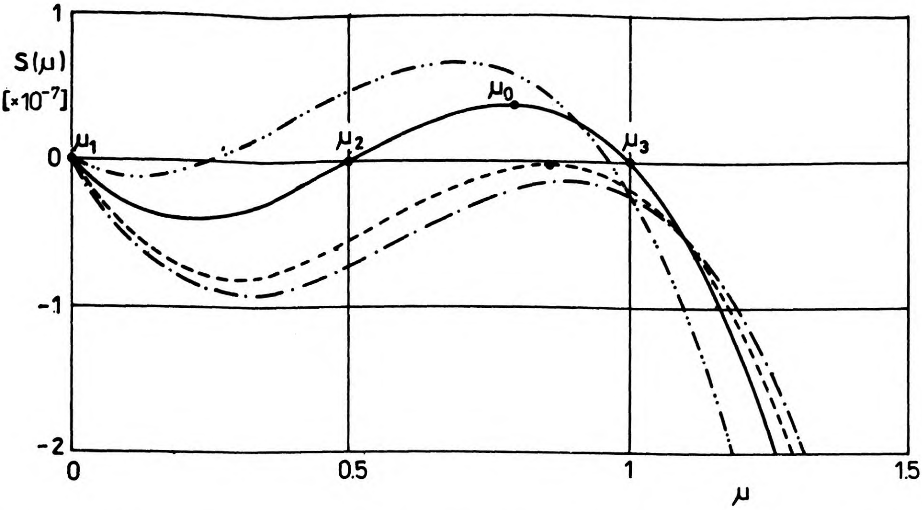

Fig. 3. Spherical aberration coefficient S in dependency of relative wavelength shift μ for selected value of parameters r and different values of parameter p (configuration No. 1)

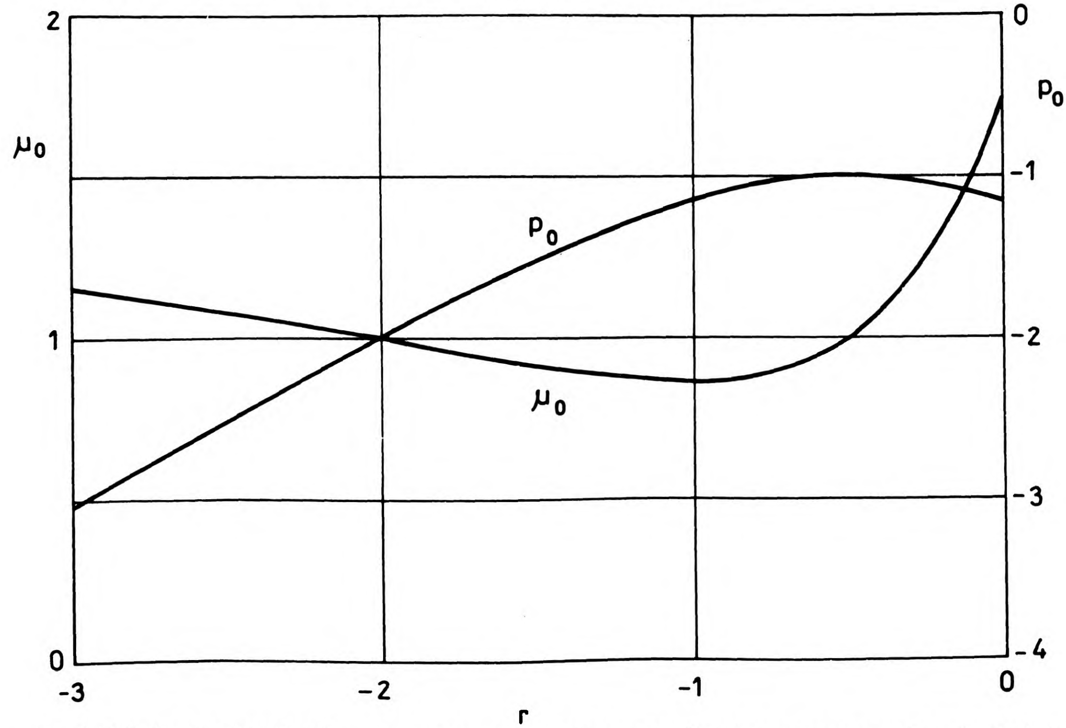

Fig. 4. Relative wavelength shift μ_0 and value of parameter p_0 assuring the best compensation of spherical aberration in dependency of parameter r (configuration No. 1)

configuration No. 1 (Fig. 2). The "base" wavelength is changed by shifting the image observation plane in this configuration.

As it can be seen from (2c), the function $S(\mu)$ has a form of third-order polynomial. The first root of this function is $\mu_1 = 0$ and is of no meaning to us. The other ones (if they exist) take the values:

$$\mu_2 = \{3p + [4(1-r^3)/(1-r) - 3p^3]/2(1-r)\}^{1/2},$$
$$\mu_3 = \{3p - [4(1-r^3)/(1-r) - 3p^3]/2(1-r)\}^{1/2}. \tag{3}$$

The graphs of $S(\mu)$ for some exemplary values of parameters r and p are presented in Fig. 3. By proper choice of these parameters the aberration free image can be obtained for desired value of μ, however, any change of the imaging light wavelength causes the appearance of spherical aberration.

As it can be seen from (2b), the function $S(\mu)$ has a local maximum for $\mu_0 = 3p/2(1-r)$, and it is possible to have simultaneously $S(\mu) = 0$ and $dS/d\mu = 0$ for some value of $\mu = \mu_0$. Parameter μ_0 determines the "optimum" observing plane location. The spherical aberration coefficient in the neighbourhood of this point varies slowly, and therefore, if the observation plane is moved off this "optimum" location then some spherical aberration apprears but it remains reasonably small

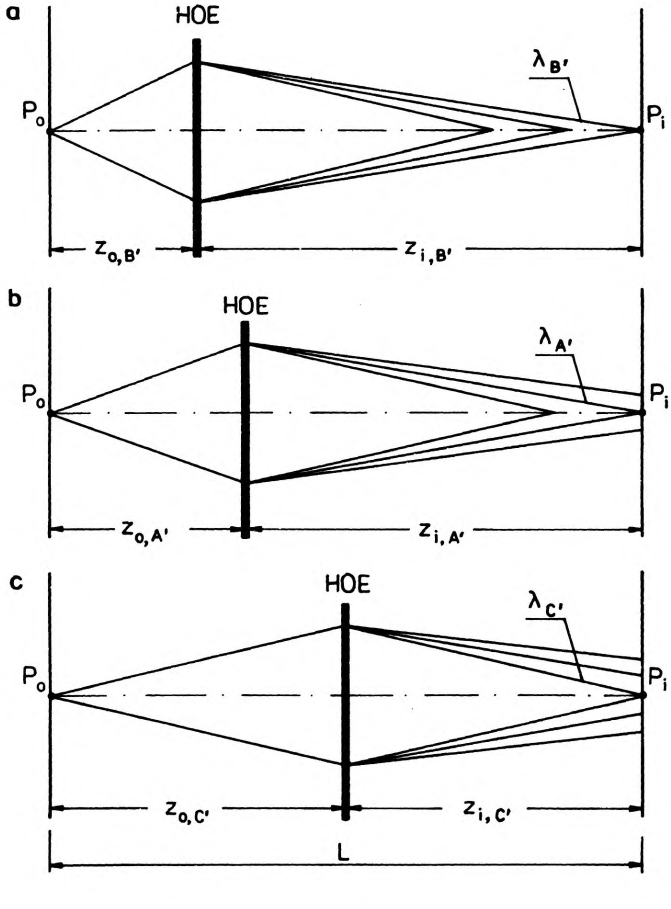

Fig. 5. Schematic diagram of spectral device in configuration No. 2: **a** – geometry B′, **b** – geometry A′, **c** – geometry C′

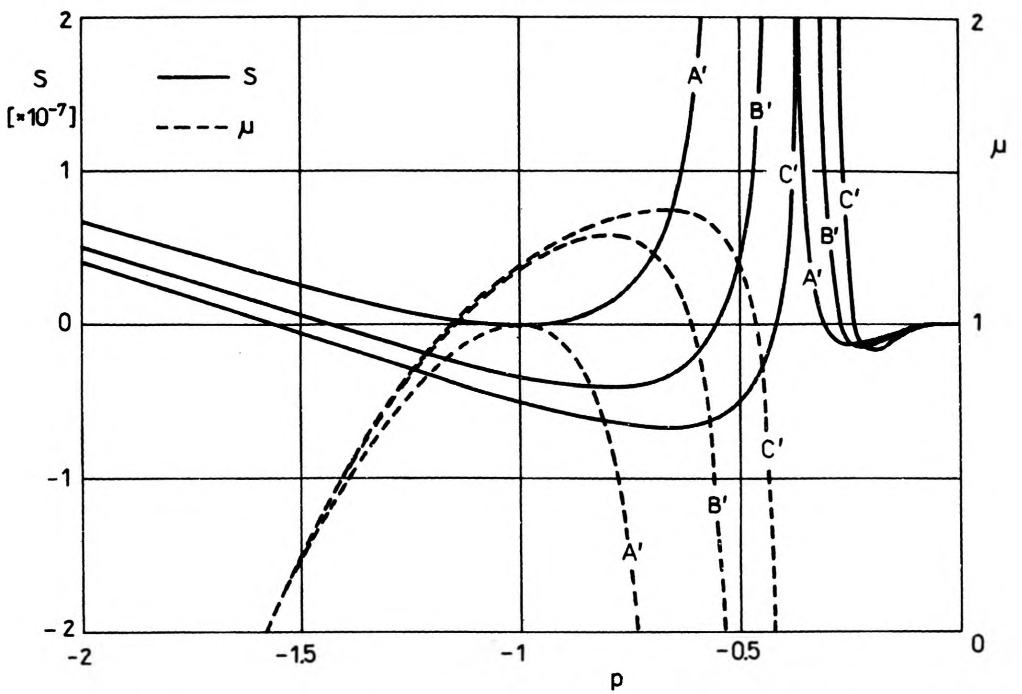

Fig. 6. Spherical aberration coefficient S and relative wavelength shift μ in dependency of parameter p for selected value of parameter r and different values of parameter w (configuration No. 1)

(dashed curve in Fig. 3). The value of μ_0 for which the best aberration compensation is achieved depends on the geometry of the holo-lens recording, as it can be seen from Fig. 4, and therefore, it can be fitted to the technology conditions.

2.3. Configuration No. 2

The imaging geometry of fixed object-image distance $z_0+z_i = z/w = \text{const}$ will be called configuration No. 2 (Fig. 5). The plane of image observation is fixed independently of the light wavelength used. By changing the location of the holo-lens along the axis between an object and fixed image plane (change of parameter p) the "base" light wavelength λ_2 creating the Gaussian image in the fixed plane is chosen.

In this configuration spherical aberration coefficient S depends on the parameter p as follows:

$$S(p) = p^2\{p-p[w/(p+w)]^3-[1/(p+w)][(1-r^3)/(1-r)]\}. \tag{4}$$

The "base" wavelength is given by

$$\mu = -p^2/(p+w)(1-r). \tag{5}$$

The graphs of $S(p)$ and $\mu(p)$ for some exemplary values of r and different values of r are presented in Fig. 6. As it can be easily seen no good image can be achieved for too big or too small value of parameter p when μ and S tend to infinity. However, one can get images of limited spherical aberration when holo-lens location is defined by the parameter p of value close to -1 for $\mu < 1$.

It would be desirable to have the condition $dS/dp = 0$ fulfilled as before. That leads to symmetrical holo-lens location ($p = -2w$) and the following spherical aberration coefficient (generally non-zero):

$$S(p = -2w) = 2p^2\{p-(1/p)[(1-r^3)/(1-r)]\}. \tag{6}$$

If the parameters p, w and μ fulfill the relations:

$$\begin{aligned} p_0 &= -[(1-r^3)/(1-r)], \\ w_0 &= 0.5[(1-r^3)/(1-r)], \\ \mu_0 &= 2[(1-r^3)/(1-r)], \end{aligned} \tag{7}$$

then, additionally, spherical coefficient S vanishes.

The imaging geometry described by those parameters (p_0, w_0, μ_0) is not convenient, however, because any shift of the observation plane (independently of its direction) results in decreasing of the coefficient μ, i.e. in no way can the Gaussian image in longer "base" wavelengths be obtained. In practice, it is better to choose another value of p_0 defining the "optimum" object distance for which some small spherical aberration appears but the $S(p)$ function changes slowly in the neighbourhood. Additionally the $\mu(p)$ function should be monotonic in the same range of parameter p variations.

3. Holo-lens spectral device

3.1. Principle of operation

The holo-lens operating as described above can be treated as a model of simple spectral device such as a spectrometer or a monochromator.

In the first application the non-monochromatic light beam whose spectral content is to be investigated illuminates a pinhole or an input slit located in the point P_o. In the observation plane distant by z_i from the holo-lens a sharp image of the pinhole in one, "base", wavelength is formed while the other wavelengths give blurred images. Therefore, the image of the input pinhole observed (or measured) in the plane P_i is coloured. This colour depends on the relative location of the input pinhole, holo-lens and image observation plane. By their shifting the analysis of the light illuminating input slit can be performed.

A monochromator can be obtained if a polychromatic (e.g., white light) point source is located at P_o, and an opaque screen with a small pinhole (exit slit) is located at P_i. Then, by proper shifting of the holo-lens or the screen the spectral content of the light flux emerging from the exit slit can be changed.

To investigate fully the optical properties of the described devices, it is necessary to evaluate the image given in polychromatic light not only when the imaging geometry corresponds to "optimum" distances z_o and z_i (denoted in the following as

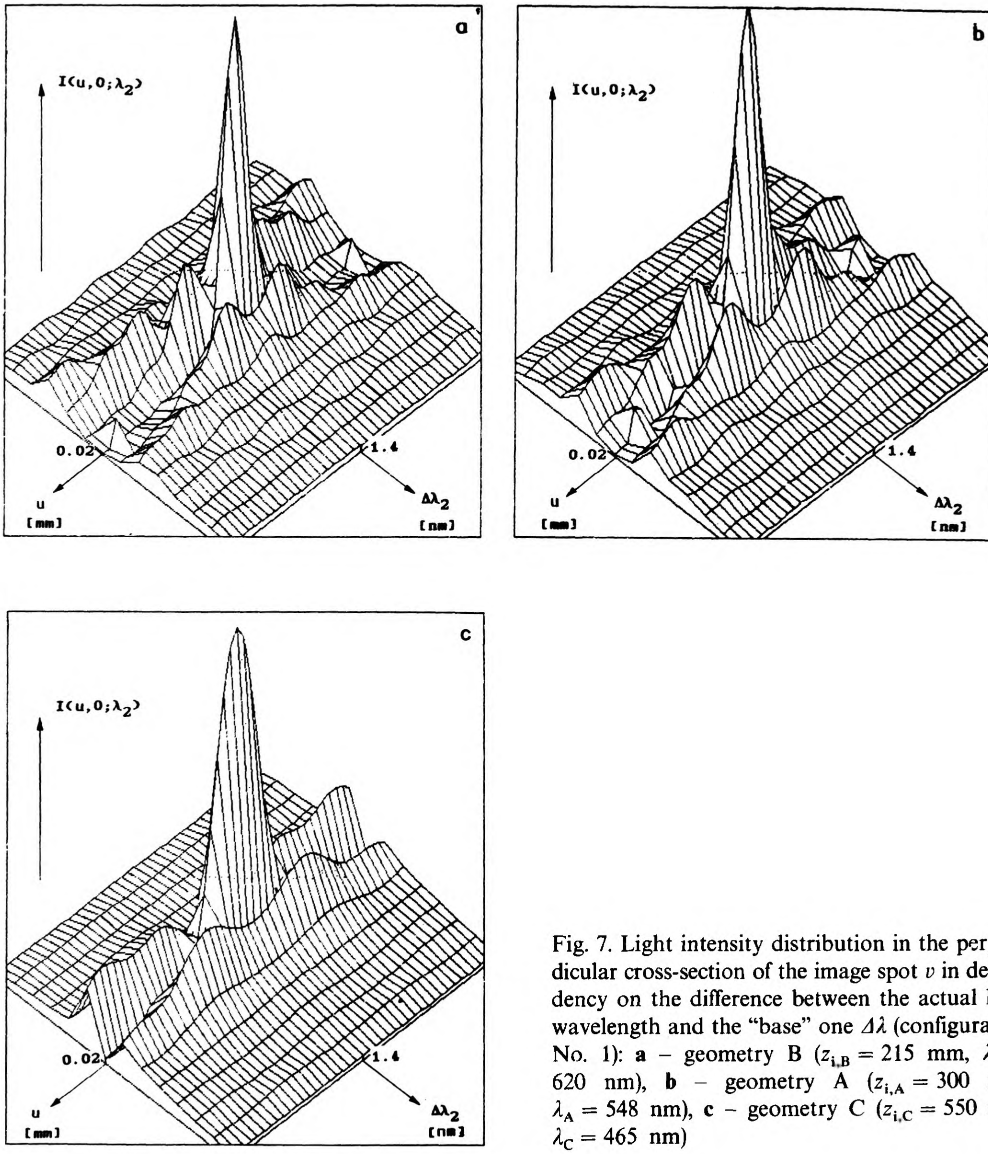

Fig. 7. Light intensity distribution in the perpendicular cross-section of the image spot v in dependency on the difference between the actual light wavelength and the "base" one $\Delta\lambda$ (configuration No. 1): **a** – geometry B ($z_{i,B} = 215$ mm, $\lambda_B = 620$ nm), **b** – geometry A ($z_{i,A} = 300$ mm, $\lambda_A = 548$ nm), **c** – geometry C ($z_{i,C} = 550$ mm, $\lambda_C = 465$ nm)

geometry A or A′) but also when the holo-lens and observing screen are relatively shifted off this position. It can be supposed that to obtain an opinion about imaging quality in the whole range of the admissible relative shifts of the holo-lens or observing screen, it is enough to examine two exemplary combinations of the object and image distances for each configuration. These values of z_o and z_i should be chosen in such a way, that the respective "base" light wavelengths are as close to the short- or long-wavelength limits of the visible light range as possible. On the other hand, it is desirable to have the spherical aberration coefficient not greater than 10^{-7} which assures that the Marechal criterion for the "base" wavelength is fulfilled. These two cases are denoted as geometry B, B′, C, C′ respectively.

3.2. Numerical investigation

For estimation of the imaging quality of the holo-lens working under the conditions described by all geometries mentioned above, the computer analysis based on the numerical evaluation of the image [10] was performed. The following recording parameters of the holo-lens for both configuration are chosen: $r = -1$, $z_\alpha = 173.2$ mm, $z_\beta = -173.2$ mm, $\lambda_1 = 632.8$ nm, $D = 30$ mm (where D is the holo-lens input pupil diameter). Then the best aberration correction is achieved for λ_2 equal

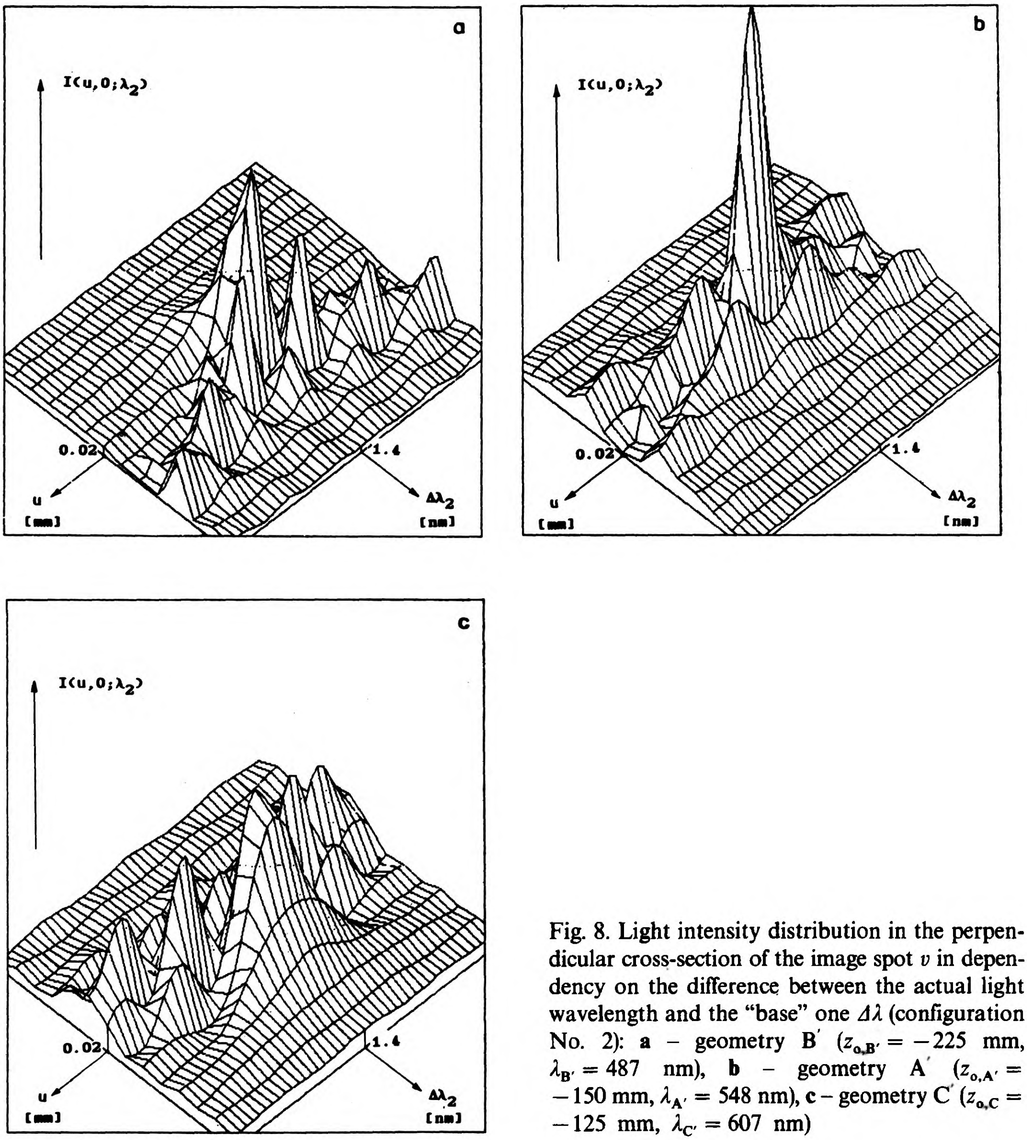

Fig. 8. Light intensity distribution in the perpendicular cross-section of the image spot v in dependency on the difference between the actual light wavelength and the "base" one $\Delta\lambda$ (configuration No. 2): **a** – geometry B′ ($z_{o,B'} = -225$ mm, $\lambda_{B'} = 487$ nm), **b** – geometry A′ ($z_{o,A'} = -150$ mm, $\lambda_{A'} = 548$ nm), **c** – geometry C′ ($z_{o,C} = -125$ mm, $\lambda_{C'} = 607$ nm)

approximately to the middle of the visible light spectrum range. The holo-lens focal length for this wavelength is $f_0 = 100$ mm. The values of object and image distances as well as "base" light wavelengths and spherical aberration coefficient S for both configurations No. 1 and No. 2 in three selected geometries are given in the Table.

Some parameters of investigated imaging

Configuration	Geometry	z_o [mm]	z_i [mm]	λ_2 [nm]	$S(\lambda_2)\times 10^{-8}$
	B	−150	550	465	−0.74
No. 1	A	−150	300	548	0
	C	−150	215	620	−1.98
	B′	−225	175	487	2.18
No. 2	A′	−150	300	548	0
	C′	−125	325	607	−17.19

To have a complex characteristic of polychromatic image formed by the anlysed holo-lens the light intensity distribution $I(u, v; \lambda_2)$ in the image of a point is calculated for λ_2 varying from $\lambda_{min} =$ 360 nm to $\lambda_{max} = 750$ nm. It was assumed that a point object emits the equal intensity for each wavelength from visible range. The results are presented in Figs. 7 and 8, where the light intensity distribution in the perpendicular cross-section v of the image spot in dependency on the difference between actual light wavelength and the "base" one $\Delta\lambda$ are shown for the geometries A, B and C (configuration No. 1, Fig. 7) and A′, B′, C, (configuration No. 2, Fig. 8).

As it is easily seen in all cases colour selectivity effect appears, the maximum of

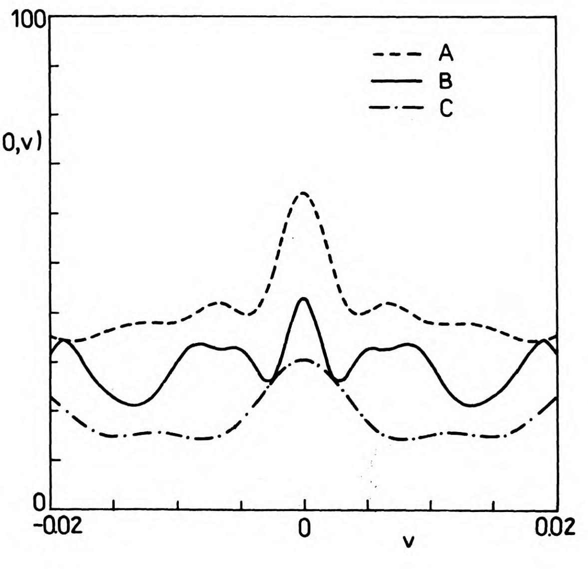

Fig. 9. Variations of illuminance across the image spot in geometries A, B, C (configuration No. 1)

the light intensity distribution curve decreases rapidly to a few per cent when λ_2 deviates from the "base" one for about $\Delta\lambda_2 = 1$ nm only.

It is interesting to evaluate the polychromatic illuminance in the image

$$\Phi(u, v) = \int_{\lambda_{min}}^{\lambda_{max}} I(u, v; \lambda)\bar{y}(\lambda)d\lambda \tag{8}$$

where $\bar{y}(\lambda)$ describes the sensitivity function of the human eye.

It appears that in all geometries A, B, C (in configuration No. 1) or A', B', C' (in configuration No. 2) a small light spot on a quite intensive homogeneous background can be observed (Figs. 9 and 10, respectively).

It could be interesting to know the colour of image of a point object emitting white equienergetic light.

To find the colour of the image the chromaticity coordinates are calculated:

$$\begin{aligned} x(u,v) &= X(u,v)/[X(u,v)+Y(u,v)+Z(u,v)], \\ y(u,v) &= Y(u,v)/[X(u,v)+Y(u,v)+Z(u,v)] \end{aligned} \tag{9}$$

where:

$$\begin{aligned} \mathrm{X}(u,v) &= \int_{\lambda_{min}}^{\lambda_{max}} I(u,v;\lambda)\bar{x}(\lambda)d\lambda, \\ \mathrm{Y}(u,v) &= \int_{\lambda_{min}}^{\lambda_{max}} I(u,v;\lambda)\bar{y}(\lambda)d\lambda, \\ \mathrm{Z}(u,v) &= \int_{\lambda_{min}}^{\lambda_{max}} I(u,v;\lambda)\bar{z}(\lambda)d\lambda. \end{aligned} \tag{10}$$

The variation of chromaticity across the image spot are maked by lines in chromaticity coordinate (x, y) distribution (Fig. 11 for configuration No. 1, and

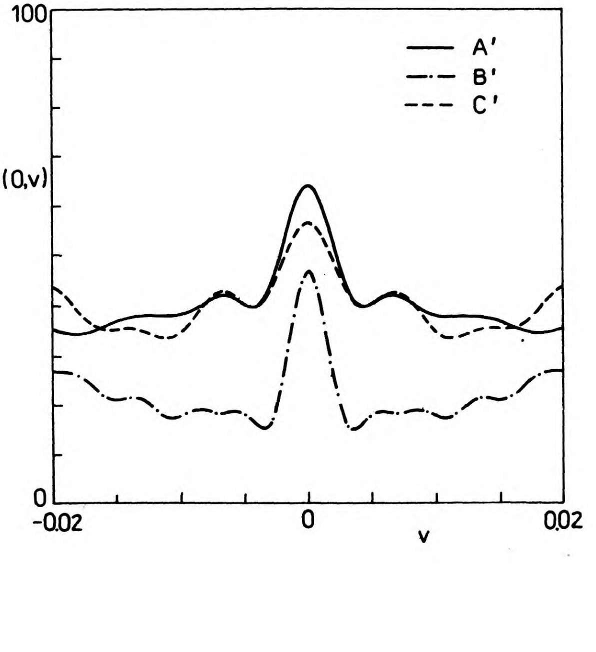

Fig. 10. Variations of illuminance across the image spot in geometries A', B', C' (configuration No. 2)

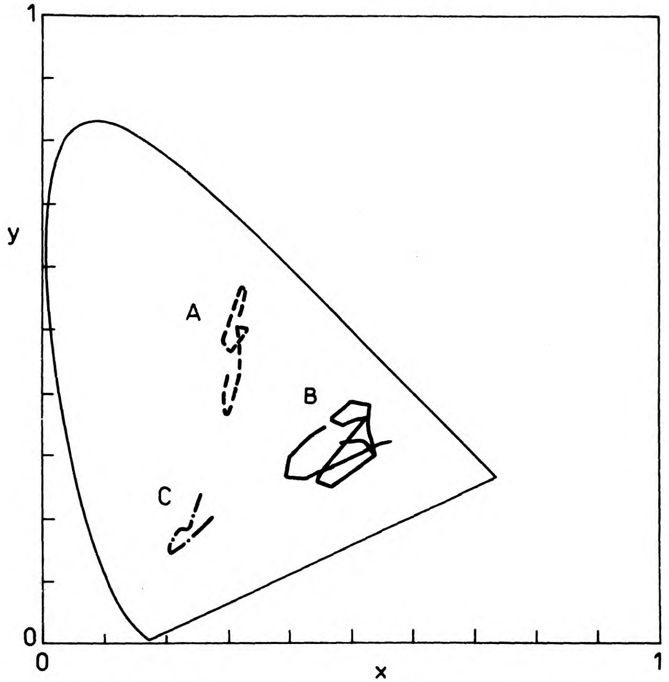

Fig. 11. Variations of chromaticity across the image spot in geometries A, B, C (configuration No. 1)

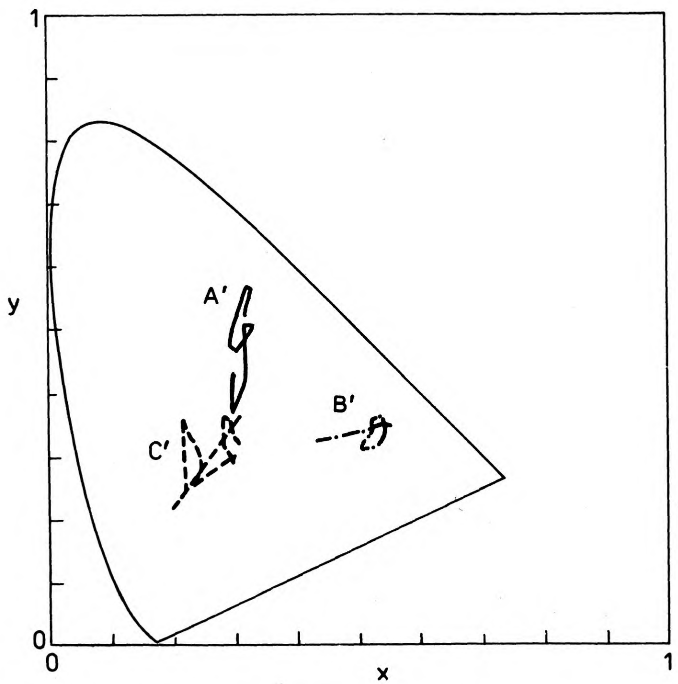

Fig. 12. Variations of chromaticity across the image spot in geometries A', B', C' (configuration No. 2)

Fig. 12 for configuration No. 2). For each chosen geometry the colour of the image spot is different. For the geometry A (or A′) yellow-green, for geometry B (or B′) red and for geometry C (or C′) blue colour spots are observed.

If an opaque screen with a small pinhole (or exit slit) is placed in the image plane, then the device acts as a kind of monochromator. To characterize its quality a spectral content of the light flux emerging from the pinhole can be useful. The relative light intensity $T(\lambda)$ can be evaluated from the following integral:

$$T(\lambda) = \iint_{\Sigma} I(u, v; \lambda)\, du\, dv \tag{11}$$

where Σ denotes the pinhole surface. The exit pinhole diameter is chosen to be approximately equal to the appropriate Airy disk diameter and equals 0.04 mm. Fig. 13 (for configuration No. 1) and Fig. 14 (for configuration No. 2) present the curves $T(\lambda)$. The peak half-width (for all examined geometries) of obtained spectral content curves varies from 3 nm to 7 nm.

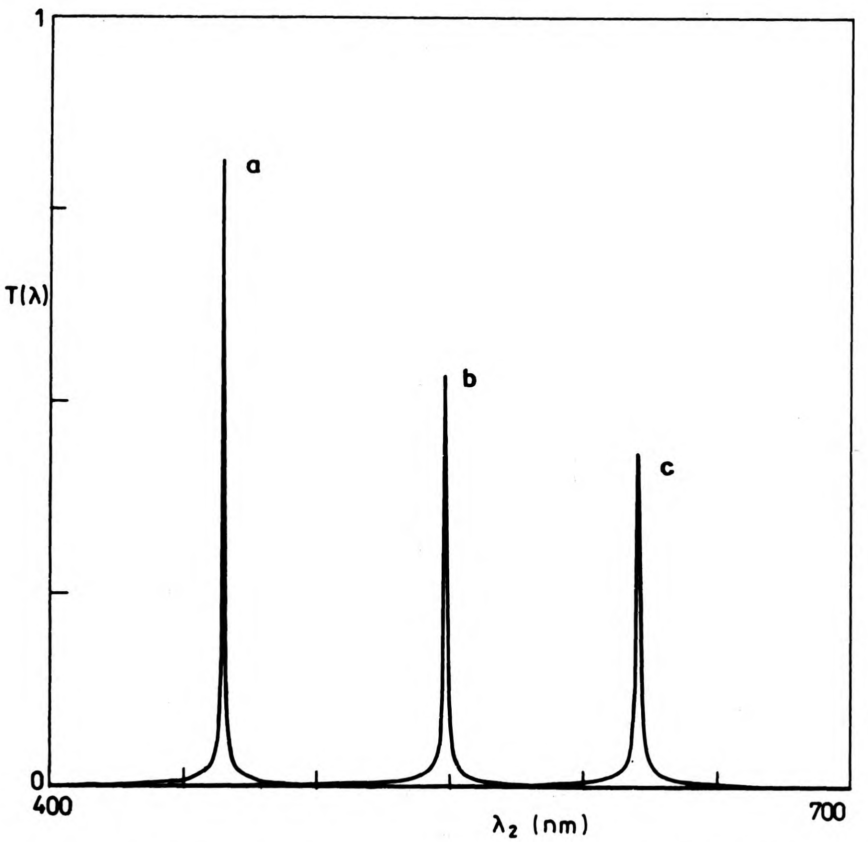

Fig. 13. Spectral content of the light flux through a pinhole located in the image plane in geometries A, B, C (configuration No. 1)

4. Concluding remarks

Holographical optical element (HOE) can be successfully used as a dispersive and imaging element simultaneously. The great chromatic aberration of HOE, in most cases regarded as a disadvantage in nonmonochromatic imaging, becomes useful in a dispersive device.

A spectral instrument such as a spectroscope or a monochromator can be built as a very simple device. An optical setup consisting of an opaque screen with an input slit, a holo-lens and an image observation screen acts as a spectroscope. This kind of spectroscope is not a common type beacuse the light spectrum is extended along z-axis, and the observation of the whole light spectrum at the same time is not possible. However, it can be designed as a scanning spectroscope, where the light spectrum is analysed by a detector moved along z-axis. A white light point source

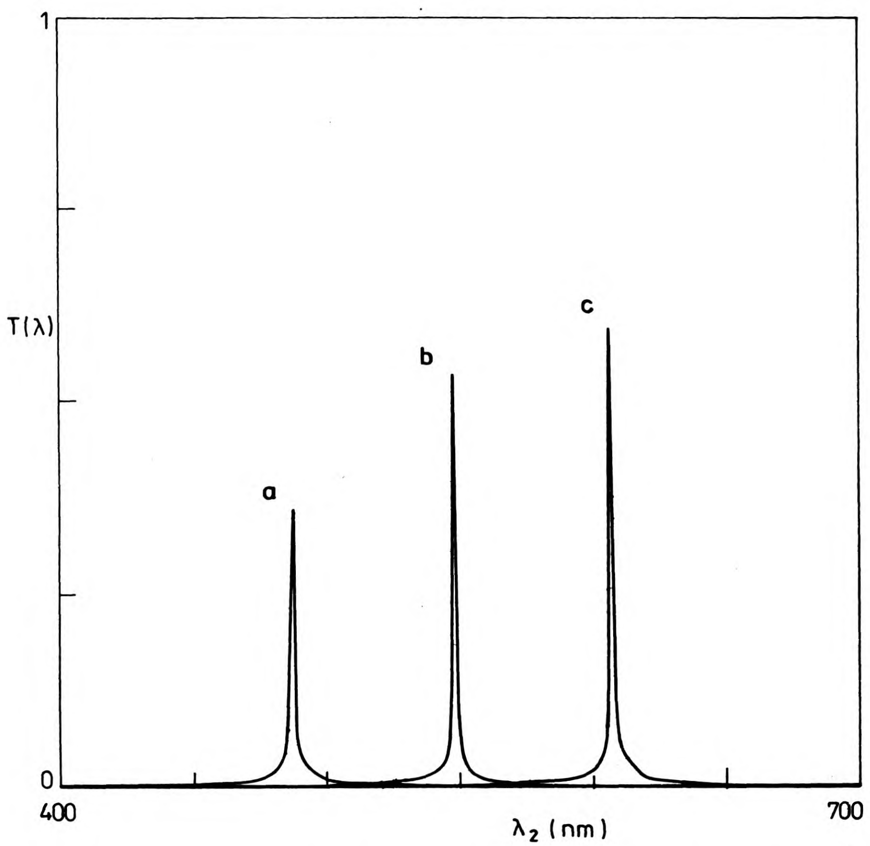

Fig. 14. Spectral content of the light flux through a pinhole located in the image plane in geometries A′, B′, C′ (configuration No. 2)

illuminating a holo-lens and an opaque screen with an output slit can be used as a monochromator. Such devices work correctly for almost the whole range of visible light spectrum. Two configurations are possible: the one of constant object to holo-lens distance enabling to obtain better imaging quality, and the other of fixed object to image distance (constant overall length) better from the technology point of view.

The computer analysis presented above needs experimental verification, that is planned for the near future.

Acknowledgements – This work has been sponsored by the Polish Ministry of National Education, Project CPBR 01. 06, and the results were presented at the IX Czechoslovak-Polish Optical Conference in Hradec na Moravici, Czechoslovakia, September 1990.

References

[1] Rallison R., Laser Appl. **3** (1984), 61.
[2] Zając M., Nowak J., Jemna Mechanika a Optika **3** (1990), 77.
[3] Pappu S. V., Opt. Laser Technol. **21** (1989), 365.
[4] Pappu S. V., ibidem p. 365.
[5] Vila R., de Frutos A. M., Mar S., Appl. Opt. **27** (1988), 3013.
[6] Zając M., Opt. Appl. **20** (1990).
[7] Zając M., Nowak J., Opt. Appl. **20** (1990).
[8] Ctyroki J., Janta J., Miler M., Skalsky M., Schrofel J., [In] *Fyzika mrizky v multiplexnim komunikacnim systemu,* (in Czech), [Ed.] M. Miler, Praha 1988, p. 49.
[9] Meier R. W., J. Opt. Soc. Am. **55** (1965), 987.
[10] Nowak J., Zając M., Opt. Acta **30** (1983), 1749.

Received November 27, 1990

О возможности коррекции сферохроматической аберрации одиночной линзы, работающей как спектральный прибор

Значительную хроматическую аберрацию, характеризующую голографическую линзу, можно использовать для получения простого спектрального устройства, в котором голографическая линза действует одновременно как дисперсный и фокусирующий элементы. Для оптимизации такого устройства необходимо проанализировать сферохроматическую аберрацию голо-линзы. В работе найдены условия для одновременного исчезновения сферической аберрации ее первой производной. Для проверки полученных формул, употребляя метод численного моделирования, определили полихроматическое изображение точечного объекта.

Проверил Станислав Ганцаж